UNIVERSITYOF BIRMINGHAM

Research at Birmingham

Laser induced ripples' gratings with angular periodicity for fabrication of diffraction holograms

Jwad, Tahseen; Penchev, Pavel; Nasrollahi, Vahid; Dimov, Stefan

Link to publication on Research at Birmingham portal

Laser induced ripples' gratings with angular periodicity for fabrication of diffraction holograms

Tahseen Jwad [a*], Pavel Penchev [a], Vahid Nasrollahi [a], Stefan Dimov [a]

∗ Corresponding author.
E-mail address: taj355@bham.ac.uk (Tahseen Jwad).

Abstract

Laser induced ripples (also known as Laser Induced Periodic Surface Structures, LIPSS) have gained a considerable attention by both researchers and industry due to their surface functionalization applications. These ripples act as diffraction gratings for the visible light therefore it is widely used in some optical applications and color marking. In this research, a method is proposed for producing holograms by varying the ripples' orientation along the beam path during the laser scanning and thus producing a pattern of ripples orientations. It was demonstrated that, by employing this method, it was possible to produce linear and radial pattern of gratings by changing the ripples' orientations following a given periodic function. As a result, smooth transitions of diffracted monochromatic light along the beam path were achieved, especially in diffracting colors from different locations when changing the azimuthal and incident angles of the incident white light. In addition, the reflection of polarized white light by such periodic gratings was investigated and it was shown that it was fully dependent on the ripples' orientations in respect to the light linear polarization vector.

Keywords: LIPSS, ripples, femtosecond laser, diffraction, selective reflection, polarization.

1. Introduction

Since laser induced ripples (also known as Laser Induced Periodic Surface Structures, LIPSS) were observed for the first time by Birnbaum [1] five decades ago, they attracted the interest of many researchers and industries due to their surface functionalization capabilities. LIPSS are considered the smallest structures that can be generated by using light [2] on most of the materials, e.g. metals, semiconductors, glasses and polymers [3, 4], and also in any environment, in particular in air, gases, liquids or vacuum [5, 6]. LIPSS have found applications in many fields including, but not limited to, brazing [7], modifying surfaces' wetting properties [8], improving surfaces' tribological performance [9-11], color marking [12-16], inhibiting bacteria attachments and facilitating cell growth [17].

In general, LIPSS have three main characteristics: depth, periodicity and orientation. The capabilities to control them become very important in the effort to produce surfaces with given functional responses. Therefore, their formation mechanism has been investigated by many

researchers in order to understand how the laser processing settings affect these three LIPSS characteristics and thus to meet the specific requirements of different applications. However, there is still no comprehensive understanding of this phenomenon [3, 4, 18] and the role of surface plasmon polaritions is still questionable [19]. From many reported empirical studies, it is evident that the LIPSS depth is nonlinearly dependent on laser fluence [20]. Regarding periodicity, LIPSS can have either low spatial frequency (LSFL) or high spatial frequency (HSFL). HSFL can be achieved using relatively low fluence [19, 21]. The periods of both LIPSS types are dependent on the laser wavelength (λ) [15]. For a normal beam incident angle, the LSFL period is approximately in the same order as λ, while for HSFL it is much smaller and depends on the material refractive index, typically $\lambda/2$ [22] or even smaller by one order [23, 24]. In case of LSFL, an increase in the laser incident angle leads to an increase of LIPSS period [25] (although some researchers have reported that the beam incident angle does not affect it [20]).

LIPSS orientation is dependent on the electric field vector of the laser polarization [20, 26]. Generally, their orientation is orthogonal to the linear polarization vector; however, LIPSS parallel to the polarization vector have been reported, too [18, 22]. Thus, the laser polarization state is very important and has a major impact on laser-matter interaction, especially on the absorbed laser energy that directly affects the damage threshold [27] and laser-matter interaction results, e.g., the width of the scanning lines [2, 28] and also the LIPSS orientation [2, 29] . Consequently, polarization state affects most of the laser-based processes such as, drilling [29-31], cutting [29, 32], welding [29] and texturing, e.g., the generation of complex surface structures [33]. Hence, the ability to control the polarization state during laser processing is important both for ablation and surface texturing applications [26].

The polarization state can be controlled employing different methods, such as using wave plates [30, 31, 34] or by employing diffractive optical elements, e.g. spatial light modulators (SLM) and liquid crystal polarizers [26, 35-38]. The effects of changing the polarization state were studied in the context of different laser processing applications, in particular, to control the orientation of nano gratings by superimposing two pulses [21]; to generate holograms inside glasses [39]; to produce polarization dependent diffraction gratings [40]; to imprint images on metallic surfaces [41]; to selectively control the appearance of two [42] or multiple symbols [13]; to generate HSFL and LSFL in one field [43]; to superimpose and overwrite LIPSS [19]; and also to generate LIPSS with different orientations within one spot using SLM [44]. Also, the influence of continuously altering the laser polarization state on drilling, sheet metal cutting and texturing operations was reported [26, 30, 31, 33, 35, 45, 46]. Recently, Hermens et al. [38] reported a synchronized use of a liquid crystal polarizer, laser scanner and 5-axis stage to generate LIPSS with different orientations on free form surfaces.

A method for producing holograms on metallic surfaces by dynamically varying the laser electric field vector is reported in this paper. In particular, a method is proposed to continuously vary the orientation of the neighboring LIPSS along the beam path by dynamically changing the orientation of a linear polarization vector during the scanning process. In this way, the LIPSS orientations within single spots or even within smaller areas (depending on the ratio between the polarization vector angular velocity and the scanning speed) were continuously varied to achieve smooth diffraction transitions along the beam path in the processed field. Then, to validate the method, linear and radial pattern of gratings were generated by following given periodic functions and scanning strategy.

2. Method

Before proceeding with the description of the proposed method, the LIPSS formation and its behavior when interacting with a white light is discussed. In particular, when ultrashort pulsed laser with fluence close to the ablation threshold interact with metal substrates, periodic ripples are generated on the surface. The period, *d*, of these ripples is mainly dependent on the laser wavelength but also on laser incident angle and dielectric constants of both the medium and the substrate as shown in Equation 1 [25, 46].

$$d = \frac{\lambda}{Re\left(\sqrt{\frac{\varepsilon_d * \varepsilon_m}{\varepsilon_d + \varepsilon_m}}\right)} \qquad \text{for normal incident angle} \qquad (1)$$

where: λ - laser wavelength, and ϵ_d and ϵ_m are the dielectric constants of the dielectric medium and the metal substrate, respectively.

Such ripples act as diffraction gratings when their periodicity is higher than the wavelength of the incident light. The diffraction order, angle and sensitivity are all dependent on the ripple periodicity and the light incident angle, as depicted in Fig.1. The functional dependence between them is as follows [47]:

$$m\lambda = d(\sin\theta_m - \sin\theta_{in}\cos\emptyset) \qquad (2)$$

where: m is the diffraction order, θ_m - diffraction angle of the m_{th} order, θ_{in} - light incident angle, and $\emptyset$ - the azimuthal angle between the grating vector and the light incident vector in the grating plane.

Ripples diffract white light when the azimuthal angle of the incident light meets specific conditions. In particular, the light is diffracted when the incident light is normal to the ripples (parallel to the LIPSS vector) in the grating plane. The intensity of the diffracted light depends on the azimuthal angle and it reaches its maximum when $\emptyset = 90°$ and drops down sinusoidally to its minimum at $\emptyset = 0°$. Thus, hologram patterns can be generated by a control rotation of polarization vector and thus make the ripple orientation dependent on their position along the beam path. However, there should also be smooth transitions of ripples' orientations across the fields and therefore the angular speed of the polarization vector rotation should be synchronized with the beam scanning speed. In this way, any abrupt changes of ripples' orientation and discontinuities across the holograms can be avoided. Since the light diffraction depends on ripples' orientations, the processed field diffracts the white light from some locations within the field but not from others when both the viewing and source angles are fixed.

Let us consider two cases of smooth light reflection across the processed fields by fixing the viewing angle. First, if the azimuthal angle of the light source varies, a smooth transition of diffracted/reflected light is achieved between neighboring spots across the processed field. Another smooth transition of the diffracted/reflected light occurs when the incident angle of the source varies. Consequently, rainbow colors associated with the first order of diffraction appear one after another because of the varying incident angle that is followed by white light reflection with zero and -1 order diffractions, respectively. Hence, changes of incident or
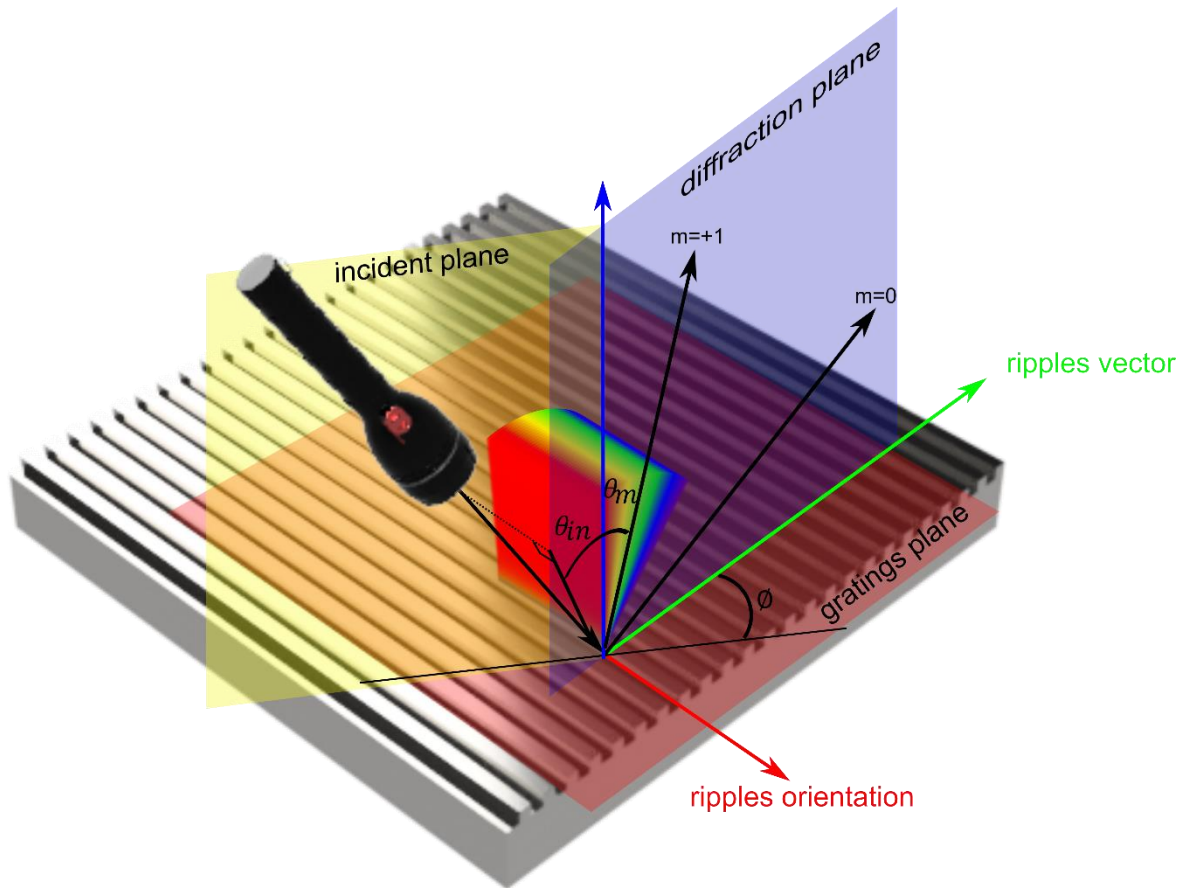
Figure 1. Interaction of white light with diffraction gratings

viewing angles lead to changes of the diffraction locations within the field and also in the diffracted colors.

As mentioned above, to generate LIPSS gratings with smooth transitions along the beam paths and thus across the processed fields, it is necessary to synchronize the angular speed of the polarization vector rotation with the beam scanning speed. The rest of the laser processing settings remain the same, in particular the scanning speed, scanning strategy, pulse repetition rate and pulse energy. It should be noted that the process settings that affect the scanning strategy (i.e., the beam scanning direction and hatch distance) also affect the resulting LIPSS gratings. The polarization vector rotation (i.e., the rotational speed of the λ/2 wave plate) could be constant, continuously varied (in particular by accelerating or decelerating it by any rate within one full revolution) or a combination of both; also, this could be implemented by setting specific time delays at every revolution or at a given number of them. Thus, by using any of the above process settings, a periodic function would be defined to repeat the LIPSS orientations at regular intervals. This function will have two variables, the ratio between the λ/2 wave plate angular speed and the beam scanning speed, and the hatch distance. A program in MATLAB was created to predict the resulting orientations along the beam path when one of these two variables is varied in the applied periodic function. The results are orientations' -matrices covering the processed field that can be depicted as images.

Since the resulting LIPSS grating is periodic, one of the variables driving this periodicity can be determined by applying the Fourier analysis. In particular, the consecutive LIPSS orientations along the beam path within the processed field would depend on the selected scanning strategy and could be represented as a vector. Then, the Fourier transform of the resulting vector can be computed to determine the respective Fourier series and periodic

function. Ultimately, this function could be used to generate the digital signal that would control the λ/2 wave plate rotation.

3. Experimental setup

To experimentally validate the proposed method, a micro processing laser platform is used; this platform integrates an Yb-doped femtoseconds laser source from Amplitude Systemes with 310 fs pulse duration, a central wavelength of 1030 nm, maximum repetitions rate of 500 kHz, and maximum pulse energy of 10 µJ. The beam delivery sub-system includes a 3D scan head (RhoThor RTA) from Newson Engineering and a 100 mm telecentric focusing lens. In particular, the input beam diameter of 5mm is focused to an irradiation spot size of 30 µm and maximum peak power of 32MW.

A setup with a motorized polarizer was designed to rotate the λ/2 wave plate with a predefined angular speed. It was implemented employing a λ/2 wave polarizer, high-precision rotation mount from Thorlabs and a NEMA 17 stepper motor to drive the polarizer through a timing belt and pulleys. The motor has 200 steps per revolution (1.8° per step) and can be controlled for up to 6400 sub-steps/revolution using a controller (TB6600) from SODIAL(R). The control signals are generated by a C programme for a Raspberry-pi3 single board computer (SBC). Fig. 2 depicts the laser processing setup used in this research and a diagram showing the polarization control sub-system.

Mirror polished stainless steel grade 304 substrates were used. The samples were ultrasonically cleaned in water and acetone and dried with hot air prior to laser processing. The processed samples were analysed employing a focus variation microscope, Alicona G5 Infinite Focus system, and a scanning electron microscope, SEM JSM-6060. Images were captured using a Nikon D3300 camera.
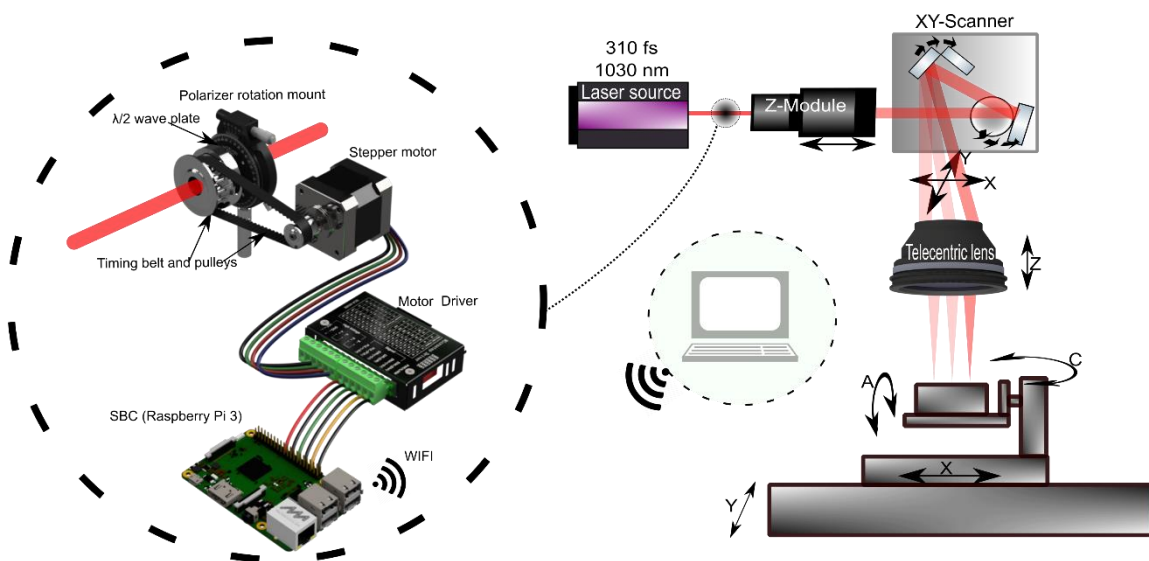

Figure 2. The laser processing platform including the implemented motorized polarizer.

3.1 Processing parameters

The most important factor affecting the ripples' generation is the laser fluence, which has to be close to the ablation threshold of the processed material. The other process settings that affect their generation are the pulse repetition rate, scanning speed and hatch distance. Some initial trials were performed to identify a suitable processing window to generate ripples' gratings on stainless steel 304 substrates. In particular, the following processing domain was identified: fluence in the range from 0.4 to 0.8 J/cm^2, number of pulses from 10 to 150 per spot, and hatch spacing in the range from 8 to 22 μm. The trials conducted showed that a higher fluence combined with a higher number of pulses and a smaller hatch distance led to darkening of the processed surface, while the opposite led to pale diffracted colors. A fluence of 0.56 J/cm^2 (a peak power of 13.5MW) and 20 pulses per spot were found to be the best to produce colorful ripples' gratings and, therefore, they were used to produce all samples in this research.

To validate the proposed method for linear pattern of ripples' orientation, a number of 10 x 10 mm^2 fields were processed with a varying ratio between stepper motor rotation and beam scanning speeds (see Supplementary Fig. S1). All the fields were produced by applying a linear zigzag scanning strategy and the process settings used to produce one of them, (see Fig 3a) are discussed further in this section 4.1. In particular, the following process settings were used to produce this field: a constant stepper motor speed of 7.8125 rev/sec achieved by sending control signals with 20 μs delays between them; and a scanning speed of 100 mm/s that resulted in a speed ratio of 28.125 deg/mm. Consequently, the ripples' orientation was repeated periodically along the beam path at every 12.8 mm within this field. The laser pulse repetition rate was kept the same, 100 KHz, and thus to maintain the number of pulses per spot at 20. Another field with a linear pattern of ripples' orientation is selected to be presented to show the selective reflection of polarized white light in section 4.3, this field was produced with a stepper motor speed to scanning speed ratio of 159.8 deg/mm along the beam path.

Another set of fields were produced but with a different processing strategy, in particular, with a circular hatching rather than the linear zigzag one. In this way, fields with a radial repetition of LIPSS orientations can be created (see Supplementary Fig. S2). One of these circular fields is shown in Fig 5a and is discussed further in this section 4.2. The diameter of the field is 10 mm and the circular hatch distance used is 12 μm. A constant stepper motor speed of 56.25 deg/sec was applied to produce this field and this was achieved by setting a delay of 1 ms between the control signals. Laser scanning speed was set at 500 mm/sec, while the pulse repetition rate was 500 KHz. LIPSS orientations are repeated along the circular path at every 3200 mm. since the scanning speed is relatively high, the processing time for this circular field was approximately 13 sec only . Another field with a circular pattern of ripples' orientation is selected to be presented to show the selective reflection of polarized white light, this circular field was processed with a varying stepper motor speed to scanning speed ratio, especially starting with 159.8 deg/mm and then decelerating it with a rate of 10 deg/mm.

4. Results

Two sets of periodic patterns with linear and radial orientations were used to validate the proposed method and then to demonstrate a selective reflection of polarized white light in the sub-sections below.

4.1. Linear periodic ripples' gratings

The effects of changing azimuthal and incident angles are clearly depicted in Fig. 3a. With the change of the azimuthal angle the diffracted light is shifted from a given location to its neighboring one in both X and Y directions. This shift is due to the LIPSS orientation effect discussed in Section 2; in particular, the incident light is diffracted predominantly from LIPSS with grating vectors parallel to the light source in the LIPSS plane and not from those normal to it. The effect of the incident angle on the appearance of the field is also depicted in Fig 3a, where three different diffracted colors are shown together with the reflected white light (near to the zero order). The effect of changing the light incident angle can be seen in the supplementary video S1. It is worth noting that the used white light source has a higher divergence; therefore, more than one color is diffracted within the same viewing angle. the modelled distribution of the LIPSS orientations across this field (referred to as an orientations' matrix in Section 2) is shown in Figure 3b.
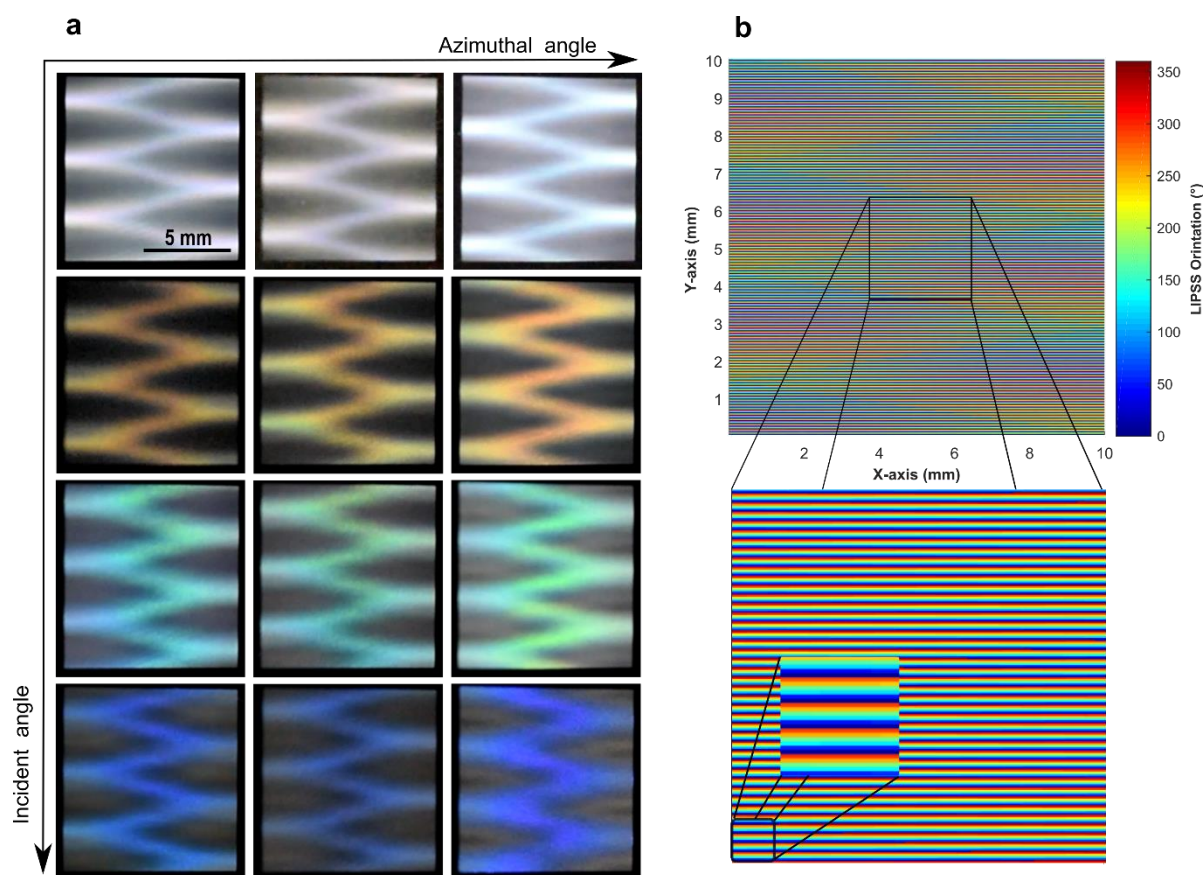

Figure 3. A ripples' field with periodic orientations: (a) the effect of azimuthal and incident angles on the diffracted light from the processed field. (b) the modelled distribution of LIPSS orientations across the field.

An SEM image of an area of 66 x 48 µm^2 within the processed field showing the changing LIPSS orientations within this field of view is given in Fig. 4. The theoretical LIPSS period should be less than the laser wavelength, approximately 1 µm (see Equation 1 above). As expected, the measured period was approximately 810 nm. Thus, the LIPSS periodicity to wavelength ratio is approximately 0.78, closed to reported ratios of 0.71 to 0.81 provided by other researchers [46]. This LIPSS periodicity of 810 nm leads to only first diffraction order of visible light wavelength spectrum (see Equation 2 above).

The overall processing time for producing the field was around 50 seconds and this could be reduced further by increasing the beam scanning and stepper motor rotational speeds or by employing a high-speed servomotor with a position feedback.
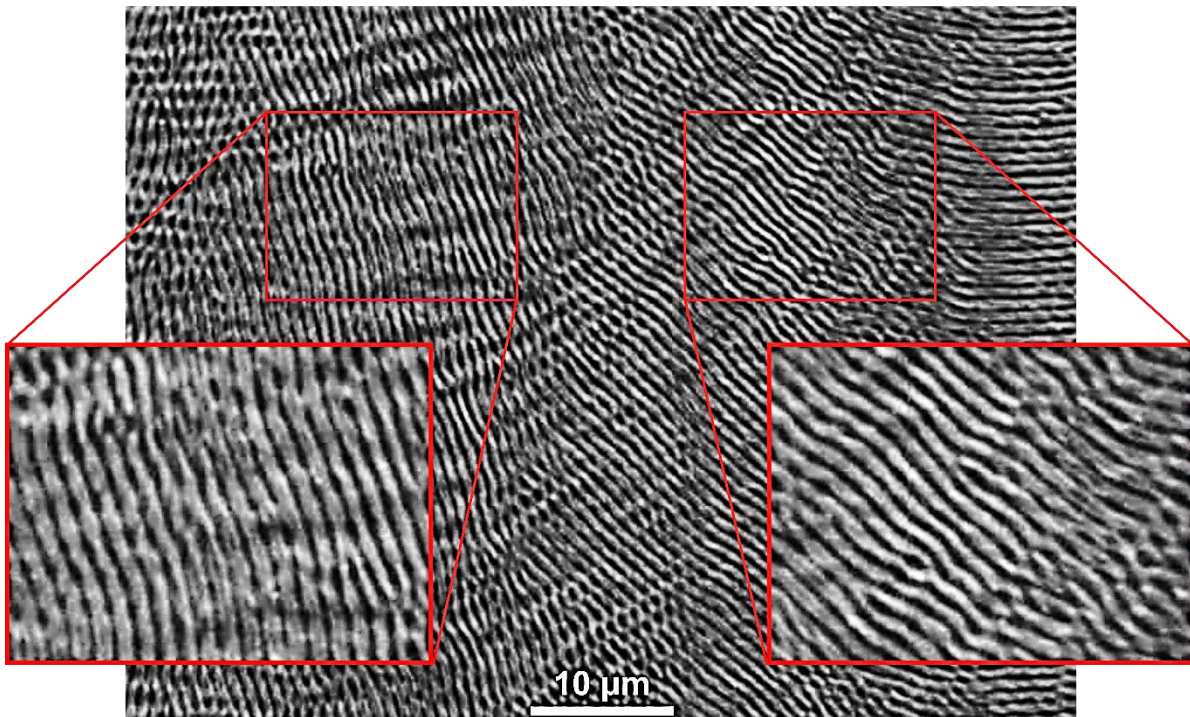

Figure 4. A SEM image of the field shown in Fig. 3a that depicts different LIPSS orientations along the beam path.

4.2. Radial periodic ripples' gratings

The effects of changing the azimuthal and incident angles are depicted in Fig 5a, while Fig. 5b represents the modelled distribution of LIPSS orientations across the circular field. As it can be seen in Fig. 5a, the shifting of the diffracted light is radial rather than cartesian. Although, the change in the polarization vector is periodic (a constant motor speed), the repetition of LIPSS orientations within the circle beam path is nonlinear. In particular, it is inversely proportional to the square of the circle radius and thus, with the increase of the radius, the frequency decreases. Also, the light diffracted from the field does not appear to be

symmetrical due to the fact that the circular scanning is not maintained across the field, in particular, it starts as circular at the field periphery and then transforms into an octagon at the centre. This can provide an additional effect to the holograms as shown in the figure. The effect of changing the source incident angles can be seen in the supplementary video S2.
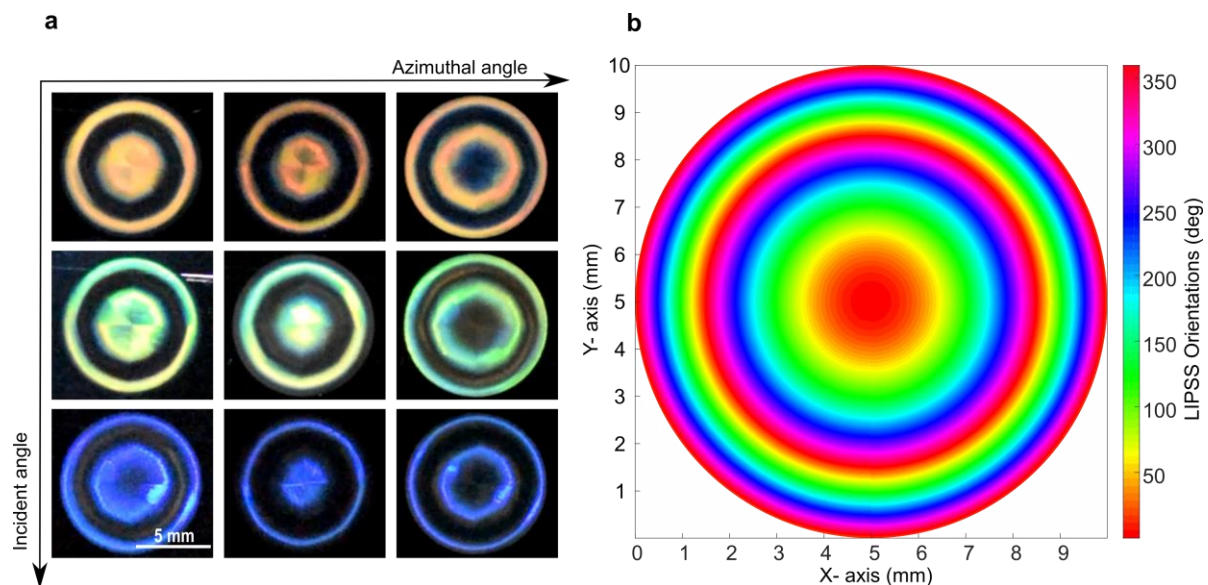

Figure 5. A grating field with radial periodic ripples' orientations: (a) the effect of azimuthal and incident angles on the diffracted white light from the same processed filed; (b) the modelled distribution of the ripples' orientations across the circular field.

4.3. The effect of white light polarization

The fields produced employing the proposed method have another interesting optical property. In particular, they reflect the polarized white light depending on the relative orientations of different areas within the field with respect to the polarization vector. This behavior is illustrated with the two fields in Fig. 6, one processed with a zigzag linear scanning strategy and the other with a circular one. The fields were viewed under the microscope using horizontal and vertical linear polarized light as shown in Fig. 6a and Fig. 6b, for the linear and in Fig. 6c and Fig. 6d for the circular, respectively. The change of the polarization vector direction led to a change of the LIPSS grating reflection. This is due to the fact that the gratings only reflect light when their polarization vector is parallel to the gratings' vector. This effect is clearer in the centre of the second circular field in Fig. 6c and 6d; in particular, the change of the polarization vector led to reflection or no reflection at the centre.
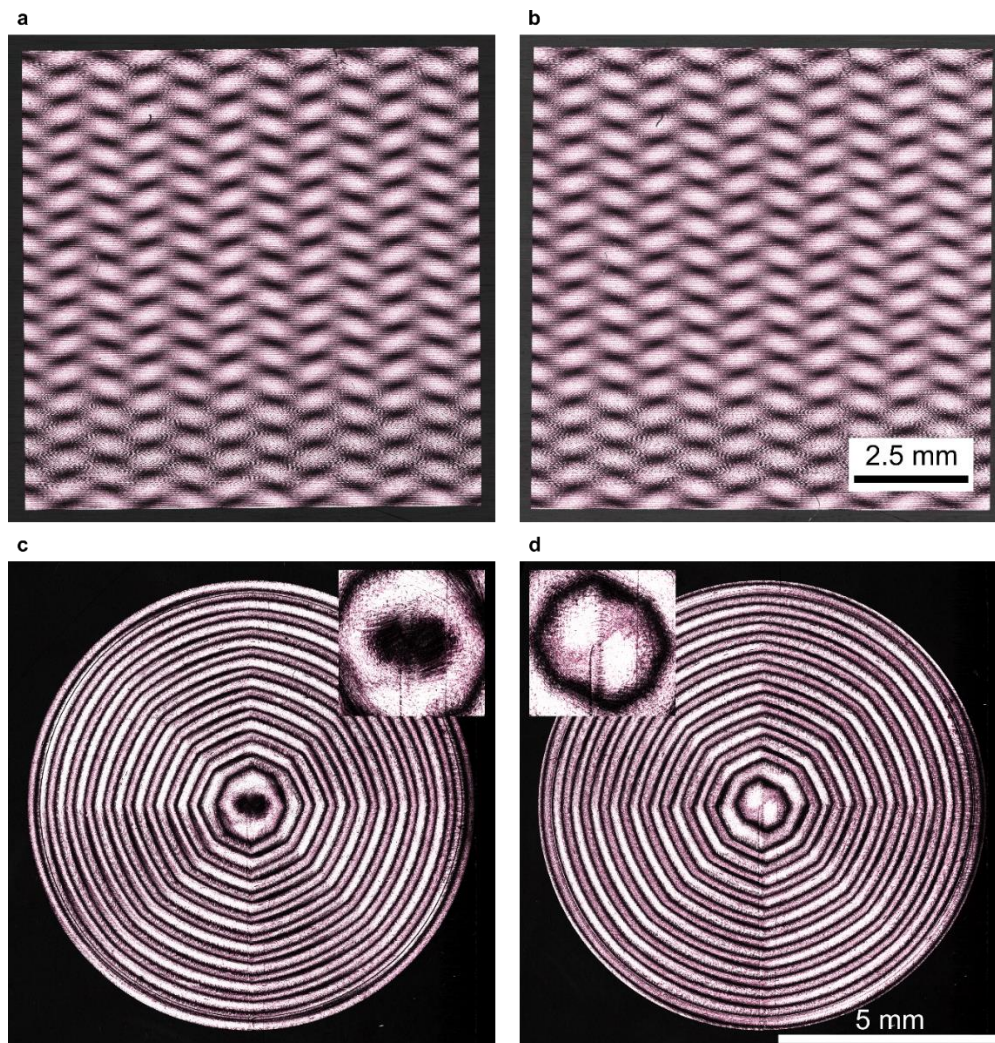
Figure 6. The fields' reflection behavior when interacting with a polarized white light: (a & b) a field processed with zigzag linear strategy reflecting vertical and horizontal linear polarized white light, respectively; (b& c) a field processed with a circular strategy reflecting vertical and horizontal linear polarized white light, respectively.

4.4. Applications

The applications of surfaces with LIPSS gratings in which orientations are varied with a given periodic function are not limited to holograms and surface color marking. Other possible applications that can be explored are the potential use of such gratings in micro fluidic systems for selective modification of wetting properties [48], in particular to create super hydrophobic tracks on surfaces and thus to direct the liquid flow along pre-defined paths. Another avenue to explore is the possibility to apply such periodic gratings in antibacterial applications [49] as some bacteria have the tendency to move along grooves. Thus, this could be inhibited by varying the LIPSS orientation with a predefined periodic function. In addition, cell migration surfaces can benefit from varied LIPSS orientations [17] and this can also be beneficial in aerodynamic and tribological applications.

Another aspect that is worth noting is that the LIPSS gratings produced with femtosecond lasers can be considered a cost-effective surface processing technology in the context of the application areas mentioned above. Bonse et al. [9] have calculated that the cost per unit area

covered with LIPSS is approximately 0.1 €/cm^2. This considers the capital investment and maintenance costs associated with the use of state of the art femtosecond laser processing systems. Recently, Gnilitskyi et al. [50] reported that it was possible to produce highly regular LIPSS with a throughput 2.5 times' faster than that reported by Bonse et al. and thus the processing time and cost could be even lower. At the same time should be noted that the relative processing cost could be reduced further if the advantages and benefits of using such functionalized surfaces are taken into account in the context of specific applications. For example, the cost of using such LIPSS gratings for improving the tribological performance of products was calculated to go down to 0.002 €/ (cm^2 × %) as the friction reduction was approximately 50% [9].

5. Conclusions

A method for producing holograms on metallic surfaces by using ripples' gratings is proposed in this research. Especially, gratings were generated where the LIPSS orientation was varied with a predefined periodic function. By applying the proposed method, linear and radial periodic ripples' gratings with angular periodicity were produced that exhibited a smooth diffraction of monochromatic light along beam path, especially reflecting different colors when changing the azimuthal and incident angles. In addition, the reflection of polarized white light by such gratings was investigated and it was shown that it was fully dependent on the LIPSS orientations in respect to the light linear polarization vector. In particular, the light was reflected only when the linear polarization vector was parallel to the LIPSS grating vector. The proposed method for producing periodic ripples' gratings could find applications in different areas, e.g. anti-counterfeiting, tribology, self-cleaning, bactericidal and cell growth enhancing surfaces, and optical applications.

References

1.   Birnbaum, M., *Semiconductor Surface Damage Produced by Ruby Lasers.* Journal of Applied Physics, 1965. **36**(11): p. 3688-&.
2.   Stankevic, V., et al., *Laser printed nano-gratings: orientation and period peculiarities.* Scientific Reports, 2017. **7**.
3.   Vorobyev, A.Y. and C.L. Guo, *Direct femtosecond laser surface nano/microstructuring and its applications.* Laser & Photonics Reviews, 2013. **7**(3): p. 385-407.
4.   Bonse, J., et al., *Laser-Induced Periodic Surface Structures-A Scientific Evergreen.* Ieee Journal of Selected Topics in Quantum Electronics, 2017. **23**(3).

5.   Albu, C., et al., *Periodical structures induced by femtosecond laser on metals in air and liquid environments.* Applied Surface Science, 2013. **278**: p. 347-351.

6.   Yang, H.D., et al., *Formation of colorized silicon by femtosecond laser pulses in different background gases.* Applied Physics a-Materials Science & Processing, 2011. **104**(2): p. 749-753.

7.   Zhang, Y., et al., *Vacuum brazing of alumina to stainless steel using femtosecond laser patterned periodic surface structure.* Materials Science and Engineering a-Structural Materials Properties Microstructure and Processing, 2016. **662**: p. 178-184.

8.   Long, J.Y., et al., *Superhydrophobic and colorful copper surfaces fabricated by picosecond laser induced periodic nanostructures.* Applied Surface Science, 2014. **311**: p. 461-467.

9.   Bonse, J., et al., *Tribological performance of femtosecond laser-induced periodic surface structures on titanium and a high toughness bearing steel.* Applied Surface Science, 2015. **336**: p. 21-27.

10.   Bonse, J., et al., *Tribological performance of sub-100-nm femtosecond laser-induced periodic surface structures on titanium.* Applied Surface Science, 2016. **374**: p. 190-196.

11.   Bonse, J., et al., *Femtosecond laser-induced periodic surface structures on steel and titanium alloy for tribological applications.* Applied Physics a-Materials Science & Processing, 2014. **117**(1): p. 103-110.

12.   Ou, Z.G., M. Huang, and F.L. Zhao, *Colorizing pure copper surface by ultrafast laser-induced near-subwavelength ripples.* Optics Express, 2014. **22**(14): p. 17254-17265.

13.   Li, J.W., et al., *Selective display of multiple patterns encoded,with different oriented ripples using femtosecond laser.* Optics and Laser Technology, 2015. **71**: p. 85-88.

14.   Vorobyev, A.Y. and C.L. Guoa, *Colorizing metals with femtosecond laser pulses.* Applied Physics Letters, 2008. **92**(4).

15.   Li, G.Q., et al., *Femtosecond laser color marking stainless steel surface with different wavelengths.* Applied Physics a-Materials Science & Processing, 2015. **118**(4): p. 1189-1196.

16.   Li, G.Q., et al., *Realization of diverse displays for multiple color patterns on metal surfaces.* Applied Surface Science, 2014. **316**: p. 451-455.

17.   Martinez-Calderon, M., et al., *Surface micro- and nano-texturing of stainless steel by femtosecond laser for the control of cell migration.* Scientific Reports, 2016. **6**.

18.   Buividas, R., M. Mikutis, and S. Juodkazis, *Surface and bulk structuring of materials by ripples with long and short laser pulses: Recent advances.* Progress in Quantum Electronics, 2014. **38**(3): p. 119-156.

19.   Gregorcic, P., et al., *Formation of laser-induced periodic surface structures (LIPSS) on tool steel by multiple picosecond laser pulses of different polarizations.* Applied Surface Science, 2016. **387**: p. 698-706.

20.   Tan, B. and K. Venkatakrishnan, *A femtosecond laser-induced periodical surface structure on crystalline silicon.* Journal of Micromechanics and Microengineering, 2006. **16**(5): p. 1080-1085.

21.   Jia, T.Q., et al., *Formation of nanogratings on the surface of a ZnSe crystal irradiated by femtosecond laser pulses.* Physical Review B, 2005. **72**(12).

22.   Bonse, J., et al., *Femtosecond laser-induced periodic surface structures.* Journal of Laser Applications, 2012. **24**(4).

23.   Sugioka, K. and Y. Cheng, *Ultrafast lasers-reliable tools for advanced materials processing.* Light-Science & Applications, 2014. **3**.

24.   Sakabe, S., et al., *Mechanism for self-formation of periodic grating structures on a metal surface by a femtosecond laser pulse.* Physical Review B, 2009. **79**(3).

25.   Ionin, A.A., et al., *Femtosecond laser color marking of metal and semiconductor surfaces.* Applied Physics a-Materials Science & Processing, 2012. **107**(2): p. 301-305.

26.   Jin, Y., et al., *Dynamic modulation of spatially structured polarization fields for real-time control of ultrafast laser-material interactions.* Optics Express, 2013. **21**(21): p. 25333-25343.

27.   Venkatakrishnan, K., et al., *The effect of polarization on ultrashort pulsed laser ablation of thin metal films.* Journal of Applied Physics, 2002. **92**(3): p. 1604-1607.

28.   Han, W.N., et al., *Continuous modulations of femtosecond laser-induced periodic surface structures and scanned line-widths on silicon by polarization changes.* Optics Express, 2013. **21**(13): p. 15505-15513.

29.   Weber, R., et al., *Effects of Radial and Tangential Polarization in Laser Material Processing.* Lasers in Manufacturing 2011: Proceedings of the Sixth International Wlt Conference on Lasers in Manufacturing, Vol 12, Pt A, 2011. **12**: p. 21-30.

30.   Nolte, S., et al., *Polarization effects in ultrashort-pulse laser drilling.* Applied Physics a-Materials Science & Processing, 1999. **68**(5): p. 563-567.

31.   Fohl, C., D. Breitling, and F. Dausinger, *Precise drilling of steel with ultrashort pulsed solid-state lasers.* Laser Processing of Advanced Materials and Laser Microtechnologies, 2003. **5121**: p. 271-279.

32.   Niziev, V.G. and A.V. Nesterov, *Influence of beam polarization on laser cutting efficiency.* Journal of Physics D-Applied Physics, 1999. **32**(13): p. 1455-1461.

33.   Skoulas, E., et al., *Biomimetic surface structuring using cylindrical vector femtosecond laser beams.* Scientific Reports, 2017. **7**.

34.   Hahne, S., B.F. Johnston, and M.J. Withford, *Pulse-to-pulse polarization-switching method for high-repetition-rate lasers.* Applied Optics, 2007. **46**(6): p. 954-958.

35.   Allegre, O.J., et al., *Complete wavefront and polarization control for ultrashort-pulse laser microprocessing.* Optics Express, 2013. **21**(18): p. 21198-21207.

36.   Cai, M.Q., et al., *Microstructures fabricated by dynamically controlled femtosecond patterned vector optical fields.* Optics Letters, 2016. **41**(7): p. 1474-1477.

37.   Hasegawa, S. and Y. Hayasaki, *Holographic Vector Wave Femtosecond Laser Processing.* International Journal of Optomechatronics, 2014. **8**(2): p. 73-88.

38.   Hermens, U., et al., *Automated polarization control for the precise alignment of laser-induced self-organized nanostructures.* Optics and Lasers in Engineering, 2018. **101**: p. 44-50.

39.   Cai, W.J., A.R. Libertun, and R. Piestun, *Polarization selective computer-generated holograms realized in glass by femtosecond laser induced nanogratings.* Optics Express, 2006. **14**(9): p. 3785-3791.

40.   Beresna, M. and P.G. Kazansky, *Polarization Diffraction Grating Produced by Femtosecond Laser Nanostructuring in Glass.* 2010 Conference on Lasers and Electro-Optics (Cleo) and Quantum Electronics and Laser Science Conference (Qels), 2010.

41.   Dusser, B., et al., *Controlled nanostructrures formation by ultra fast laser pulses for color marking.* Optics Express, 2010. **18**(3): p. 2913-2924.

42.   Yao, J.W., et al., *Selective appearance of several laser-induced periodic surface structure patterns on a metal surface using structural colors produced by femtosecond laser pulses.* Applied Surface Science, 2012. **258**(19): p. 7625-7632.

43.   Ji, X., et al., *Femtosecond laser-induced cross-periodic structures on a crystalline silicon surface under low pulse number irradiation.* Applied Surface Science, 2015. **326**: p. 216-221.

44.   Lam, B., J. Zhang, and C. Guo, *Generation of continuously rotating polarization by combining cross-polarizations and its application in surface structuring.* Optics Letters, 2017. **42**(15): p. 2870-2873.

45.   Allegre, O.J., et al., *Real-time control of polarisation in ultra-short-pulse laser micro-machining.* Applied Physics a-Materials Science & Processing, 2012. **107**(2): p. 445-454.

46.   Graf', S. and F.A. Muller, *Polarisation-dependent generation of fs-laser induced periodic surface structures.* Applied Surface Science, 2015. **331**: p. 150-155.

47.   Hecht, E., *Optics*. 4th ed. 2002, Reading, Mass.: Addison-Wesley. vi, 698 p.

48.   Wu, B., et al., *Superhydrophobic surfaces fabricated by microstructuring of stainless steel using a femtosecond laser.* Applied Surface Science, 2009. **256**(1): p. 61-66.

49.   Cunha, A., et al., *Femtosecond laser surface texturing of titanium as a method to reduce the adhesion of Staphylococcus aureus and biofilm formation.* Applied Surface Science, 2016. **360**: p. 485-493.

50.   Gnilitskyi, I., et al., *High-speed manufacturing of highly regular femtosecond laser-induced periodic surface structures: physical origin of regularity.* Sci Rep, 2017. **7**(1): p. 8485.
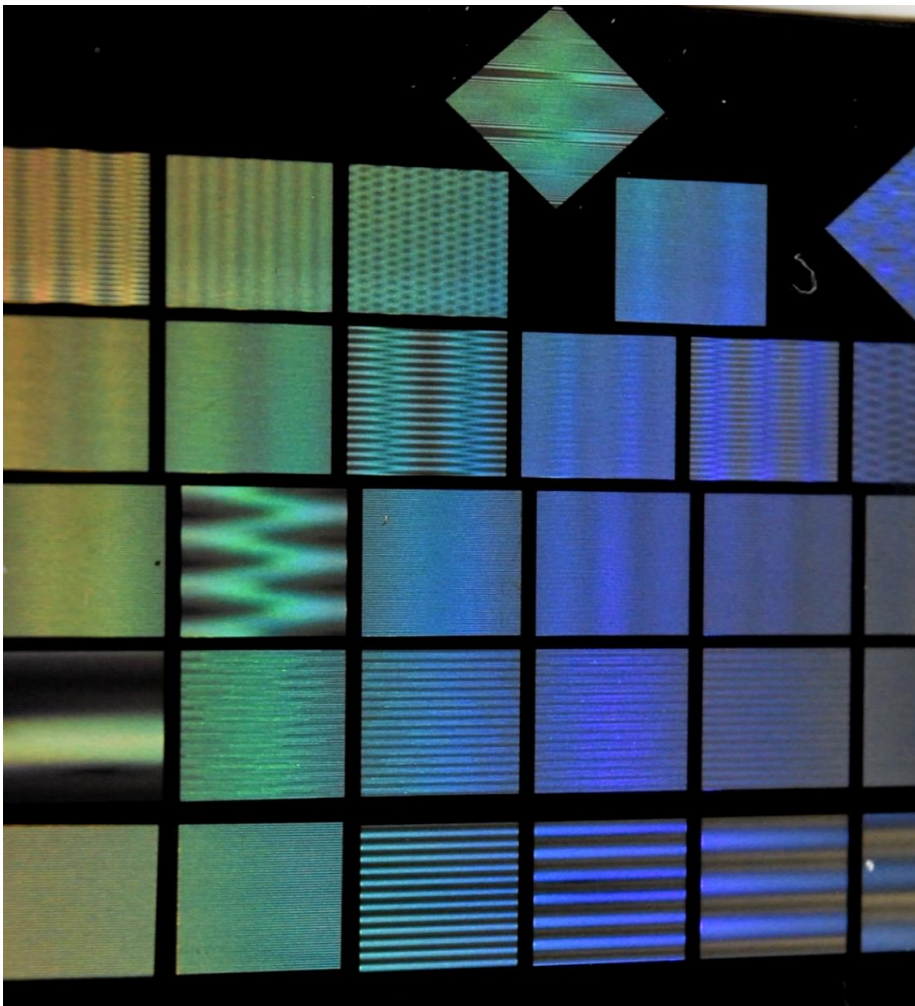
Figure S1. Fields of linear periodic pattern of ripples orientations processed with different stepper motor rotation to beam scanning speeds ratios.

Figure S2. Fields of radial periodic pattern of ripples orientations processed with different stepper motor rotation to beam scanning speed ratios.